https://doi.org/10.2352/issn.2169-2629.2021.29.328

Perceptual Navigation in Absorption-Scattering Space

Davit Gigilashvili*, Philipp Urban*,†, Jean-Baptiste Thomas*, Marius Pedersen*, Jon Yngve Hardeberg
*** Norwegian University of Science and Technology, Department of Computer Science; Gjøvik, Norway***
† Fraunhofer Institute for Computer Graphics Research IGD; Darmstadt, Germany

Abstract

Translucency optically results from subsurface light transport and plays a considerable role in how objects and materials appear. Absorption and scattering coefficients parametrize the distance a photon travels inside the medium before it gets absorbed or scattered, respectively. Stimuli produced by a material for a distinct viewing condition are perceptually non-uniform w.r.t. these coefficients. In this work, we use multi-grid optimization to embed a non-perceptual absorption-scattering space into a perceptually more uniform space for translucency and lightness. In this process, we rely on A (alpha) as a perceptual translucency metric. Small Euclidean distances in the new space are roughly proportional to lightness and apparent translucency differences measured with A. This makes picking A more practical and predictable, and is a first step toward a perceptual translucency space.

Introduction

Translucency is one of the major appearance attributes [1]. The transport of light through materials has a considerable impact on how the objects made of them look. We interact with translucent materials, such as wax and marble, on a daily basis, and generating an adequate translucent look is important in a broad range of fields, such as computer graphics, 3D printing and aesthetic medicine. [2] Subsurface transport of light is described by the *radiative transfer equation*, where a material is defined by the following intrinsic parameters: absorption and scattering coefficients, scattering phase function, and index of refraction, all of which are wavelength-dependent. Absorption (σ_a) and scattering (σ_s) coefficients correspond to the average distance in inverse scene units a photon travels inside the material before getting absorbed or scattered, respectively. *Mean free path* is the average distance a photon travels in a straight line without being scattered and absorbed, and is equal to $\frac{1}{\sigma_a+\sigma_s}$. Phase function defines the distribution of the directions a photon is redirected to after scattering. Index of refraction describes the speed of light in a material and the angle the light path is bent with at the boundary of the materials with mismatching indices of refraction.

Appearance of objects can be changed by modification of the optical properties of the materials they are made of. However, the link between the change in optical properties and the resulting appearance change is not fully understood [2], and getting a desired visual look oftentimes requires a trial-and-error approach, which is costly and time-consuming. Creating a system that permits us to navigate through objectively measurable quantities with an awareness of its perceptual consequences can considerably speed-up and simplify this process. One important quality this kind of system needs to possess is perceptual uniformity – steps made in this system should be, to some extent, proportional to resulting changes in perceptual qualities. For instance, perceptual uniformity of color spaces has long been a topic of scholarly interest [3]. There have been attempts to create a perceptually uniform gloss space [4] as well as various perceptual embeddings for gloss [5, 6]. Unlike color spaces, knowledge on translucency spaces remains limited. Apart from the work by Gkioulekas *et al.* [7], which focuses on one parameter – in particular, phase function, no perceptually uniform translucency space has been proposed to date [8]. Gigilashvili *et al.* [9, 10] observed that absorption-scattering space is highly non-uniform from the perceptual perspective – equal changes in absorption and scattering coefficients produce different magnitude of changes in apparent translucency in different parts of the space.

A (alpha) – a simplified one-dimensional representation of translucency that is nearly perceptually uniform was recently introduced by Urban *et al.* [11]. They conducted phsychophysical experiments on a set of virtual homogeneous materials to measure a psychometric function that links optical properties of a material with the magnitude of translucency perceived by humans when observing this material under fixed illumination conditions. The virtual materials possess an isotropic phase function, refractive index of 1.3, and are parametrized by wavelength-independent scattering and absorption coefficients (the properties of the materials and the viewing conditions *A* was defined for can be found in ***Supplementary Material 1***[1]). *A* is software- and hardware-independent, and encapsulates knowledge about many peculiarities of translucency perception by humans – for instance, *A* accounts for the phenomenon that subtle changes in absorption and scattering are detected easily when the magnitude of absorption and scattering is low, while the translucency difference may not be noticeable between two highly scattering materials, even if the Euclidean distance between them in the absorption-scattering space is large.

Although Urban *et al.* [11] provide a software implementation for calculating *A* for each pair of σ_a and σ_s coefficients, perception-aware navigation in the absorption-scattering space remains a cumbersome task, because for computing A-distances between two points in the absorption-scattering space, *A* needs to be computed for each point separately. As perception-aware navigation in absorption-scattering space is non-Euclidean, in this work, we attempt to create a tabulated space where Euclidean distances are perceptually more meaningful. We propose taking advantage of ΔA (difference in *A*) as an objective apparent translucency difference metric and use it for modifying the absorption-scattering space in such a way that the Euclidean distances (ΔD) in a new space are roughly proportional to changes in object's appearance. We would like to emphasize that the aim is to construct a space to be used for small ΔA only. Small differences are of special interest, as the large distances can be picked and distinguished easily, while fine tuning for small distances (or constructing uniform gradients) is a more cumbersome task.

For this purpose, we use a method based on multi-grid optimization, similar to the one introduced in [12]. It is important to consider that σ_a and σ_s do not only affect translucency

[1] All supplementary materials can be downloaded from www.colorlab.no/cid and www.igd.fraunhofer.de/en/publications

– an increase in σ_a and σ_s also affects lightness of the materials, making them darker or lighter, respectively [2, 11]. Materials with the same A might considerably differ in lightness. For this reason, instead of projecting the materials to 1-dimensional A-space, we define a 2-dimensional nearly perceptually uniform translucency-lightness space. By *nearly perceptually uniform* we mean that the Euclidean distances in this space are roughly proportional to "perceptual distances" measured for nearly perceptually uniform scales of "Lightness CIE-L*" and "A". ΔA is limited to a comparison between particular materials, while instant conversion to the space proposed by us enables faster and more perception-aware navigation in the physical parameter space.

We want to highlight that this work does not provide a translucency appearance space with adjustable viewing conditions. The major objective of this work is to enable more perception-aware navigation in physical parameter space under fixed viewing conditions primarily for graphical 3D printing applications. Although this work concerns with virtual homogenous materials, A is meaningful both optically and perceptually, making it applicable to real heterogeneous materials [11].

The paper is organized as follows: in the next section we describe the technical details of the optimization process. Afterwards, we introduce and discuss the resulting space. In the subsequent section, we analyze the limitations of the work. Finally, we conclude and propose future research directions.

Methodology

Multigrid optimization technique

In order to conduct the perceptual embedding, we relied on the method proposed by Urban *et al.* [12], which is based on the multi-grid optimization technique (also see [13]). The authors provided an isometric embedding of non-Euclidean color spaces into Euclidean color spaces. Although the methodology is primarily intended for color spaces, it can be used for translucency as well, as long as a reliable translucency difference metric is available. The principle of the optimization is the following (illustrated in Figure 1): the original space is covered with two grids, where each node of the inner grid is surrounded by the four nodes of the other grid. In the preliminary step, the perceptual differences (P1-P4) are found between each node and its four enclosing neighbors. The goal of the optimization is to move the nodes in such a way that the distances between the nodes and each of its neighbor are as close as possible to a fixed parametric distance (which is perceptual, in this case). For a given node $K_{x,y}$ of one grid (red in Figure 1), which is enclosed by four nodes of the other grid (blue in Figure 1), $K_{x,y}$ should be displaced in a way that the disagreement between the perceptual (P1-P4) and the Euclidean (D1-D2) distances is minimized. It is important to mention that the perceptual differences are calculated just once, in the beginning of the process, while the Euclidean distances are calculated on each iteration, i.e. after each displacement. The objective function that needs to be minimized is given as follows:

$$F(k_{x,y}) = \sum_{i=1}^{4} (P_i - D_i)^2 = min \tag{1}$$

Gradient descent is used to identify the direction of the steepest descent and the enclosed node is displaced towards that direction. The magnitude of the displacement is defined with the *step size*. It is, however, critical that after displacement, a given node remains enclosed with its original neighbors to preserve order in the grid. This process is repeated over multiple iterations. Once all nodes of the inner grid are displaced, then the nodes of the outer grid are displaced with the same principle. The nodes

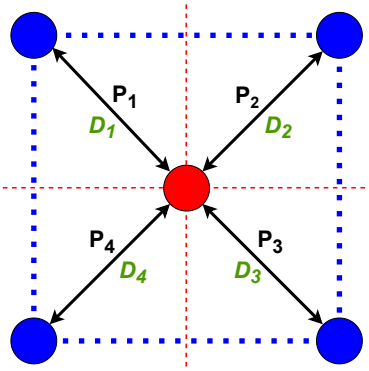

Figure 1. *The goal of the optimization is to move a red node to the location, where the disagreement between the perceptual differences (P1-P4) and the Euclidean distances in the space (D1-D4) is minimal. The new location must be within the same four quadrilateral formed by the 4 blue nodes.*

located on the edges and at the corners of the outer grid move relative to two or one neighbor(s) of the inner grid, respectively. The nodes of the outer grid that are located on the axes move across these axes only (1-dimensional displacement), while the origin ([0;0]) remains fixed. The optimization stops either after a pre-defined number of iterations, or according to a specific termination criterion. Eventually, the original and the final locations of the nodes are used to construct a look-up table (LUT) that will permit conversion from the original space to the coordinates of the resulting space by means of bilinear interpolation. Each node of the LUT is defined as follows:

$$k^0_{x,y} \mapsto k^N_{x,y} \tag{2}$$

where $k^0_{x,y}$ is the position of node of the original grid (zero iteration); $k^N_{x,y}$ is the position of the same node after N iterations.

The backward transform from the new space to the original absorption-scattering space is possible using scattered interpolation that relies on a Delaunay triangulation [14]. The lookup tables as well as the MATLAB scripts and respective instructions for instant conversion between the two spaces can be found in *Supplementary Material 2*.

Optimization process

The range from 0 to 203 cm^{-1} in absorption-scattering space[2] was covered with two rectangular grids with dimensions of 36×36 and 35×35 (203 was selected for a practical reason: A becomes 0.99 and increasing σ_a and σ_s further affects A only negligibly; thus, all values higher than that will be concatenated down to 203 in the conversion process). The outer grid at iteration 0 was sampled equidistantly in the logarithmic scale, to ensure that the grid is denser in optically thin regions (low σ_a and σ_s) and sparser in optically thicker ones (high σ_a and σ_s), as in the optically thin regions the visual system is more sensitive to σ_a-σ_s differences. The dimensions of the grid (36×36) was carefully selected with the same factor in mind – the distances among the neighboring nodes should be neither too short (so that they were indistinguishable visually), nor too large (as the perceptual difference metrics, discussed below, are defined for small differences only). Each vertex of the inner grid was initiated as a mean among the four surrounding vertices of the outer grid. After this initialization, a numerical optimization was conducted for each enclosed vertex. Optimizing a 36×36 grid from scratch is

[2] All σ_a and σ_s coefficients in this work are in cm^{-1} units.

computationally costly. To speed up the process, we used multi-scale optimization. Initially, we sampled a 3×3 grid composed of the 1st, 19th, and 36th nodes of the original grid. 3×3 was optimized for 10000 iterations. The resulting LUTs have been used to convert a 5×5 grid to the new space (composed of the 1st, 8th, 19th, 27th, and 36th nodes of the original grid). The optimization continued with this 5×5 grid. The grid was gradually made denser, to 9×9, 17×17, and eventually 36×36. On each round, the optimization was run for 10000 iterations, unless the following termination criterion was met:

IF *Disagreement* $<= \frac{1}{scale^3 \times 1000}$

BREAK;

where *Disagreement* is a mean disagreement between the perceptual and Euclidean distances among all nodes of the inner grid; *scale* is an arbitrary parameter, proportional to the denseness of the grid, *scale*=1 for 3×3 and *scale*=5 for 36×36.

The disagreement in the resulting 36×36 grid was still large. Therefore, it was iterated for further 1.2 million iterations, where it gradually converged to a stable state. The *step size* was adapted manually, depending on the convergence speed and varied in the range of 0.001-0.00005. Termination tolerance was set to 1e-6 for the whole process.

Selection of a perceptual metric

In order to construct such a space, it is essential to have an adequate measure of perceptual differences. Unlike color difference, no widely accepted perceptual translucency difference metric exists. ΔA – the absolute difference in A cannot be used directly as there is no bijectivity between σ_a- σ_s and ΔA. There exist trajectories in the σ_a- σ_s space with constant A (see constant A curves in Figure 3 of [11]). Along these trajectories $\Delta A = 0$. For instance, materials with high σ_a and low σ_s, and low σ_a and high σ_s can possess identical A, while the Euclidean distance between them is large.

To avoid this problem, we considered lightness information in combination with σ_a and σ_s. As mentioned above, absorption and scattering have qualitatively different effect on lightness for the considered viewing condition (4mm thick patch, white backing etc. – see ***Supplementary Material 1***). Even if translucency (A) is equal, highly absorbing materials look dark, while highly scattering materials look brighter. There exists unique mapping between [A;L*] and [σ_a; σ_s]. Besides, lightness (L* of the CIELAB) itself significantly affects the appearance of translucent materials. For these reasons, we concluded that building a perceptually uniform space based solely on A is infeasible, and decided to create a combined translucency-lightness space based on A and L* (the details of the lightness measurements can be found in ***Supplementary Material 1***). The perceptual difference metric encapsulates a combined difference in A and L*. For combining the differences in two essentially dissimilar parameters, we took an approximate just noticeable difference (JND) as an anchor, which is approximately equal to 0.1 for A [11, 15] and 1 for lightness [15, 16]. Eventually, we came up with the following perceptual difference metric ΔP:

$$\Delta P = \sqrt{(0.1 \times \Delta L^*)^2 + \Delta A^2}, \quad (3)$$

where $\Delta L^* = |L_1^* - L_2^*|$ and $\Delta A = |A_1 - A_2|$.

Results

The absorption-scattering space in the range of 0-203 was embedded into another space that is roughly given in the range of 0-1. Although ΔP can take values from 0 up-to approximately 10, the space is constructed for small differences only and is not intended to accommodate such large differences.

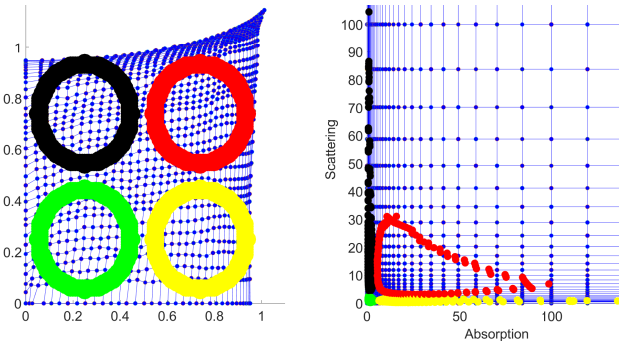

Figure 2. *The left image illustrates the generated perceptual Euclidean space, while the right image shows a portion of the absorption-scattering space. Points with the same colors in the two spaces correspond to the same materials that illustrates the deformations between the spaces. Four perfect circles covering most of the perceptual space (left image) actually correspond to a small, optically thin part of the absorption-scattering space, while most of the absorption-scattering space is embedded into a dense top right corner of the resulting space. Consider that roughly only a quarter of the absorption-scattering space is shown in the image, in order to make all points corresponding to the circles in the left image visible. The shapes in the absorption-scattering space are not continuous due to the sparse sampling in the new space. A high resolution version of this figure can be found in* ***Supplementary Material 3.***

The constructed space largely exhibits the characteristics of A – the absorption and scattering space is distorted by the embedding so that the Euclidean distances in optically thin regions are increased and in optically thick regions decreased. The perceptual space is skewed towards the increasing direction of the axes. In other words, the grid is sparse in the lower end, and becomes increasingly denser as we move to the positive direction of the axes. This means that a larger part of the absorption-scattering space is mapped to a small range of high values in the resulting space. This behavior was expected, because human observers are more sensitive to absorption-scattering differences when their magnitudes are small, while differences between highly scattering media are harder to distinguish [9, 10]. This is illustrated in Figure 3 of [11], which shows that increase in absorption and scattering produces larger non-distinguishable areas. If the area in the absorption-scattering space is non-distinguishable, the distances in the resulting space should be minimal that explains high density of the grid in these areas, as a broader range of absorption-scattering coefficients need to be "squeezed" into a smaller area of the resulting space. This is illustrated in Figures 2 and 3. Figure 2 illustrates four perfect circles with a radius of 0.2 in the resulting Euclidean space. If we convert the respective coordinates back to the absorption-scattering space, we will see that the four circles that cover most of the area in the produced space correspond to merely smaller sub-region of the absorption-scattering space, characterized with relatively low absorption and scattering. On the other hand, Figure 3 illustrates three smaller circles in the dense part of the resulting space with radii equal to 0.02, 0.015, and 0.01. When converted back to the absorption-scattering space, we observe that these tiny sub-regions in the new space are actually embeddings of a large hardly distinguishable regions in the absorption-scattering space. Another interesting observation is the fact that the points located on perfect circles in the produced space, yield highly non-uniform droplet-like contours in the absorption-scattering space.

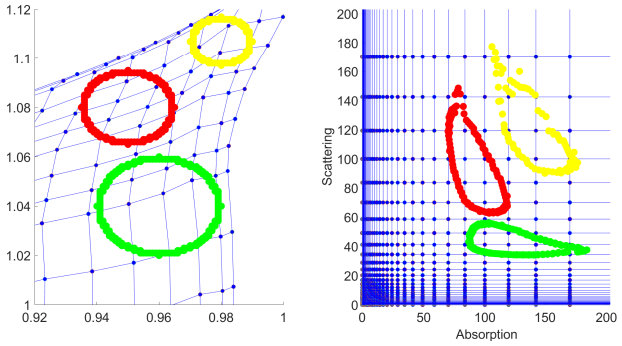

Figure 3. *Large regions of hardly-distinguishable translucent and opaque materials (right image) are embedded into a very dense but small region of the grid (left image). We observe that the circles in the perceptual space (left) are highly skewed in the absorption-scattering space (right), which once again highlights the non-uniformity of the absorption-scattering space. The shapes in the absorption-scattering space are not continuous due to the sparse sampling in the new space. A high resolution version of this figure can be found in* ***Supplementary Material 3.***

Figures 4 and 5 show absorption-scattering and resulting spaces, respectively. The locations of the renderings of the Stanford Lucy objects correspond to that of the material they are rendered with. A and lightness values are also shown for each image. Figure 4 shows that the absorption-scattering space is uniform neither in terms of A, nor in terms of lightness. Steps in the absorption-scattering space do not correspond to the resulting A and L* differences. In the resulting space, the images seem to be grouped by lightness, and the distances within the groups roughly correspond to ΔA, meaning that the space is roughly uniform locally. It should be mentioned that as the embedding is optimized w.r.t small differences in A and L*, some groups of the Lucy materials are rather far away from each other in the space. We believe that in this case a multidimensional scaling would create a higher degree of uniformity.

We are interested to know how erroneous our embeddings are, and how the tension is distributed in the grid – whether it is evenly distributed (small error in all areas), or concentrated in a particular region (large error in a particular part of the grid). In order to assess the quality and accuracy of the embedding, we generated 10 000 random pairs of materials with $\Delta P < 0.2$ (the perceptual difference metric is only reasonable locally, for small differences). We calculated the disagreement between ΔP and ΔD in the resulting space for each of those pairs. The summary statistics of the disagreements over 10 000 random pairs is given in Table 1. Disagreement is measured with two metrics: the absolute difference between ΔP and ΔD; and this difference relative to ΔP, calculated as:

$$\frac{|\Delta P - \Delta D|}{\Delta P} \tag{4}$$

Although average and median disagreement values seem acceptable, there are some pairs producing unexpectedly high disagreement. We sorted the pairs by their disagreement values and noticed an interesting trend: the vast majority of the pairs producing high disagreement fall under those two categories (examples are given in Table 2):

1. Scattering coefficient of one of the materials is very low (Example 1 in Table 2). It seems that the tension is concentrated in this area that can be ascribed partly to the fact that the nodes on the axes were fixed and could not move in 2D, and partly to the sparsity of the grid in this region.
2. ΔA is negligibly small between two nearly opaque materials. On the one hand, this permits the optimization process to locate those points very close to one another; while, on the other hand, the lightness differences as small as $\Delta L^* = 2$, are enough to produce the disagreement in the range of 0.2 (Example 2 in Table 2). As mentioned above, our perceptual metric is valid for small differences only. As each node was compared only with its immediate neighbors in the optimization process, we assumed that ΔL^* would not be much larger than the JND. However, a dense concentration of the nodes from different parts of the original grid, corresponding to opaque highly scattering materials, produced some pairs that are less than 0.2 units away in the resulting Euclidean space, while having lightness differences considerably larger than the JND.

Table 1: The summary statistics of the absolute and relative disagreements observed between 10 000 random pairs in the original absorption-scattering and the new perception-aware spaces. The table shows that the disagreement between perceived and Euclidean differences is orders of magnitude smaller in the new space compared to the absorption-scattering space. The absolute differences in the new space, except for a small subset of pairs, are low; relative differences are higher than absolute ones. They are mostly lower than 1, indicating that perceptual metric differences are oftentimes larger than the distances in the dense part of the grid.

	Original σ_a-σ_s space		In the new space	
	Absolute	Relative	Absolute	Relative
Mean	50.75	540.51	0.07	0.63
Median	43.15	430.65	0.07	0.67
Max.	191.49	4.08E+03	0.44	6.92
99th Pct.	152.01	2.33E+03	0.18	0.99
Min.	0.47	5.38	7.49E-06	2.83E-04
Std	36.32	466.03	0.05	0.27

Limitations

Considering that ΔA plays an essential role in the optimization process, the resulting space inherently suffers from all limitations of A. In particular, A was measured on simple homogeneous virtual materials that have wavelength-independent σ_a and σ_s, fixed index of refraction and an isotropic phase function. However, A can be estimated for a real heterogeneous material as well *"by minimizing a distance function between light transport measurements of this material and simulated measurements of the reference materials"* [11] conducted by a commercial spectrophotometer. Also, A assumes perfectly smooth surface and does not incorporate surface scattering effects caused by rough surfaces, which also affects translucency [2, 17]. Furthermore, as ΔA is perceptually meaningful for small A differences only, the space is only locally uniform in terms of perception, i.e. ΔD in our space is roughly proportional to the perceptual difference if and only if ΔD is small. A similar limitation is characteristic to color difference formulae as well, that are usually meaningful for small to medium color differences only [18, 19]. We foresee that the method used by us will be also valid for future refined expressions of A or similar measures of perceptual translucency.

We realize that our perceptual metric (Eq. 3) needs a psychophysical validation in the future, as a linear combination of

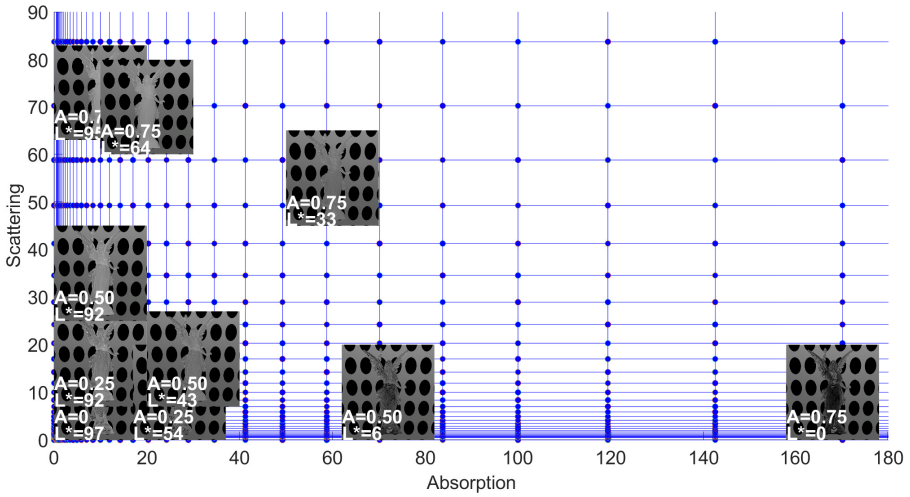

Figure 4. *The renderings are located in the absorption-scattering space at the position of the respective materials they are rendered with. The numbers on the images report respective A and lightness values. It is apparent that absorption-scattering space is highly non-uniform in terms of both of those parameters. A high resolution version of this figure can be found in* ***Supplementary Material 3****. Please, note that the materials shown here are equidistantly sampled in terms of A, but not in terms of L*; therefore, they are not expected to be equidistant in the new space either.*

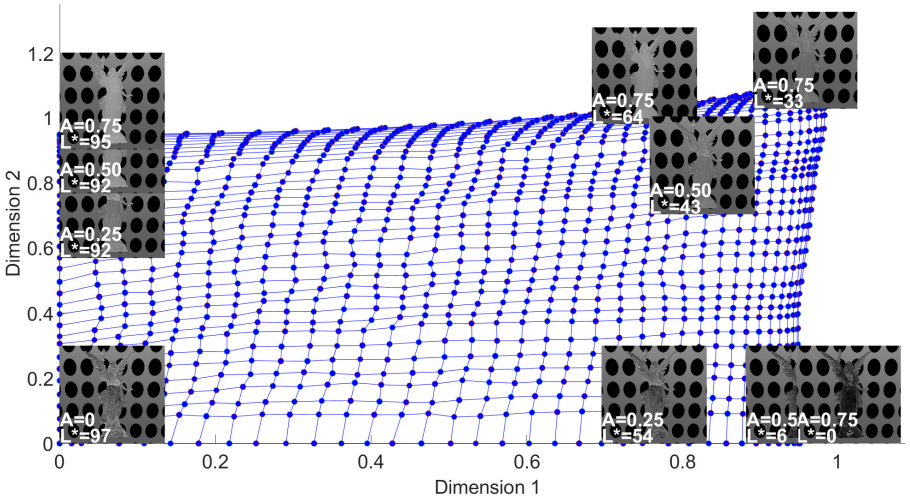

Figure 5. *The location of the renderings in the pseudo-uniform Euclidean space. Materials with moderate and high absorption and scattering are pushed towards the extremes. They are grouped by lightness and ΔD within these groups seem more proportional to A differences than in the absorption-scattering space. A high resolution version of this figure can be found in* ***Supplementary Material 3.*** *Please, note that these materials were not selected to be equidistant in lightness; thus, it is not a surprise that they are not uniformly distributed in the new space.*

different perceptual measures might not yield a robust perceptual metric. However, the approach is promising as a similar method has been successfully used by Chen and Urban [15] to combine A with CIEDE2000 color difference in deep learning applications.

A is defined under fixed viewing conditions. Hence, we want to highlight that we created a translucency-lightness space for a fixed viewing condition and it should not be thought of as an appearance model where viewing conditions can be adjusted. We realize that accommodating broader range of materials and conditions are essential to generic applicability of the resulting space. However, this requires a rigorous re-definition of A metric, which is beyond the scope of this work. As the first step toward this direction, the primary objective of this work has been to facilitate the navigation in absorption-scattering space limited to the materials A is defined on. However, if validated psychophysically and refined accordingly in the future, the space has a potential to develop toward a more generic appearance model.

Finally, perceived translucency difference depends not only on material, but also the shapes of the objects that are being compared [9, 10]. Adjustments are needed to accommodate these shape-related effects currently not accounted for by ΔA.

Conclusions and Future Work

The physical absorption-scattering coefficient space is perceptually highly non-uniform. We conducted a multi-grid optimization and constructed a 2-dimensional perception-aware space for translucency and lightness. With *perception-aware* we mean that the Euclidean distances in this space are roughly proportional to the ”perceptual distances” measured for nearly perceptually uniform scales of ”Lightness CIE-L*” and ”A”. This space facilitates navigation in the physical parameter space of absorption and scattering, which, if generalized to broad enough range of materials and conditions, can save considerable amount of resources in material design in computer graphics and 3D printing applications. Being limited to simple materials and fixed viewing conditions leaves room for future improvement.

Table 2: Examples of the material pairs producing large errors. If scattering coefficient is too small, the disagreement can be large, because the grid is sparse, and $\Delta D > \Delta P$. Contrarily, it can happen that two highly scattering materials are very close in the Euclidean space, while the perceptual difference is large due to lightness differences.

	Example 1	**Example 2**
Point 1 [abs; scat]	17.28; 3.95	76.16; 176.36
Point 2 [abs; scat]	18.46; 0.25	77.70; 158.82
Point 1 in New space	0.72; 0.58	0.94; 1.100
Point 2 in New Space	0.71; 0.05	0.94; 1.099
L*1	51.24	46.54
L*2	50.67	44.57
$\Delta L*$	0.57	1.97
ΔA	0.05	0.007
ΔP	0.08	0.197
ΔD **(in the new space)**	0.52	0.001
Disagreement (absolute)	0.44	0.196
Disagreement (relative)	5.49	0.992

First, we believe it is important to validate the perceptual metric (Eq. 3) experimentally. Second, future works should accommodate chromatic materials, different indices of refraction and anisotropic phase functions, such as those in [7]. In the long term, we also foresee the development of more sophisticated translucency difference formulae, which, in contrast with ΔA, will have parametric factors accounting for shape- [9, 10] and illumination-related [20, 21] effects on perceptual difference.

Acknowledgments

The study has been funded by the MUVApp (#250293) project of the Research Council of Norway.

References

[1] CIE 175:2006, "A framework for the measurement of visual appearance," *International Commission on Illumination,*, p. 92 pages, 2006.

[2] Davit Gigilashvili, Jean-Baptiste Thomas, Jon Yngve Hardeberg, and Marius Pedersen, "Translucency perception: A review," *Journal of Vision*, vol. 21, no. 8:4, pp. 1–41, 2021.

[3] Philippe Colantoni, Jean-Baptiste Thomas, and Alain Trémeau, "Sampling CIELAB color space with perceptual metrics," *International Journal of Imaging and Robotics*, vol. 16, no. 3, pp. 1–22, 2016.

[4] Fabio Pellacini, James A Ferwerda, and Donald P Greenberg, "Toward a psychophysically-based light reflection model for image synthesis," in *Proceedings of the 27th annual conference on Computer graphics and interactive techniques*. ACM Press, 2000, pp. 55–64.

[5] Josh Wills, Sameer Agarwal, David Kriegman, and Serge Belongie, "Toward a perceptual space for gloss," *ACM Transactions on graphics (TOG)*, vol. 28, no. 4, pp. 1–15, 2009.

[6] Matteo Toscani, Dar'ya Guarnera, Giuseppe Claudio Guarnera, Jon Yngve Hardeberg, and Karl R Gegenfurtner, "Three perceptual dimensions for specular and diffuse reflection," *ACM Transactions on Applied Perception (TAP)*, vol. 17, no. 2, pp. 1–26, 2020.

[7] Ioannis Gkioulekas, Bei Xiao, Shuang Zhao, Edward H Adelson, Todd Zickler, and Kavita Bala, "Understanding the role of phase function in translucent appearance," *ACM Transactions on graphics (TOG)*, vol. 32, no. 5, pp. 1–19, 2013.

[8] Davit Gigilashvili, Jean Baptiste Thomas, Jon Yngve Hardeberg, and Marius Pedersen, "On the nature of perceptual translucency," in *8th Annual Workshop on Material Appearance Modeling (MAM2020)*. Eurographics Digital Library, 2020, pp. 17–20.

[9] Davit Gigilashvili, Philipp Urban, Jean-Baptiste Thomas, Jon Yngve Hardeberg, and Marius Pedersen, "Impact of shape on apparent translucency differences," in *Color and Imaging Conference*, Paris, France, October 2019, Society for Imaging Science and Technology, pp. 132–137.

[10] Davit Gigilashvili, *On the Appearance of Translucent Objects: Perception and Assessment by Human Observers*, PhD thesis, Norwegian University of Science & Technology, June 2021.

[11] Philipp Urban, Tejas Madan Tanksale, Alan Brunton, Bui Minh Vu, and Shigeki Nakauchi, "Redefining A in RGBA: Towards a standard for graphical 3D printing," *ACM Transactions on Graphics (TOG)*, vol. 38, no. 3, pp. 1–14, 2019.

[12] Philipp Urban, Mitchell R Rosen, Roy S Berns, and Dierk Schleicher, "Embedding non-Euclidean color spaces into euclidean color spaces with minimal isometric disagreement," *The Journal of the Optical Society of America (JOSA) A*, vol. 24, no. 6, pp. 1516–1528, 2007.

[13] Ingmar Lissner and Philipp Urban, "Toward a unified color space for perception-based image processing," *IEEE Transactions on Image Processing*, vol. 21, no. 3, pp. 1153–1168, 2011.

[14] Isaac Amidror, "Scattered data interpolation methods for electronic imaging systems: a survey," *Journal of Electronic Imaging*, vol. 11, no. 2, pp. 157–176, 2002.

[15] Danwu Chen and Philipp Urban, "Deep learning models for optically characterizing 3D printers," *Optics Express*, vol. 29, no. 2, pp. 615–631, 2021.

[16] Bernhard Hill, Th Roger, and Friedrich Wilhelm Vorhagen, "Comparative analysis of the quantization of color spaces on the basis of the CIELAB color-difference formula," *ACM Transactions on Graphics (TOG)*, vol. 16, no. 2, pp. 109–154, 1997.

[17] Morgane Gerardin, Lionel Simonot, Jean-Philippe Farrugia, Jean-Claude Iehl, Thierry Fournel, and Mathieu Hébert, "A translucency classification for computer graphics," in *Material Appearance 2019, Electronic Imaging*. 2019, pp. 203:1–203:6, Society for Imaging Science and Technology.

[18] M Ronnier Luo, Guihua Cui, and Bryan Rigg, "The development of the CIE 2000 colour-difference formula: CIEDE2000," *Color Research & Application*, vol. 26, no. 5, pp. 340–350, 2001.

[19] WS Mokrzycki and M Tatol, "Colour difference ΔE- A survey," *Machine Graphics and Vision*, vol. 20, no. 4, pp. 383–411, 2011.

[20] Roland W Fleming and Heinrich H Bülthoff, "Low-level image cues in the perception of translucent materials," *ACM Transactions on Applied Perception (TAP)*, vol. 2, no. 3, pp. 346–382, 2005.

[21] Bei Xiao, Bruce Walter, Ioannis Gkioulekas, Todd Zickler, Edward Adelson, and Kavita Bala, "Looking against the light: How perception of translucency depends on lighting direction," *Journal of Vision*, vol. 14, no. 3:17, pp. 1–22, 2014.